Carbonaceous adsorbents from single and mixed rubber and plastic wastes. Adsorption of methylene blue

Cesar Troca-Trenado[1], María Alexandre-Franco[1], Carmen Fernández-González[1], Manuel Alfaro-Domínguez[2], Vicente Gómez-Serrano[1,*]

[1]Department of Organic and Inorganic Chemistry, Faculty of Science,University of Extremadura, Avda. de Elvas s/n, E-06006-Badajoz, Spain

[2]Derpartment of Mechanical, Energetic and Materials Engineering, University of Extremadura, Avda. de Elvas s/n, E-06006- Badajoz, Spain

ABSTRACT

From rubber of used tires (TR), plastic bottle(PET) and automobile industry EPDM/PP rubber/plastic (VR) both separately and as 1:1 binary and 6:1:1 ternary mixtures, carbonaceous adsorbents (CAs) were first prepared by heat treatment at 900 ºC in N_2 or at 850 ºC in steam, then characterized by the adsorption of N_2 at -196 ºC and mercury porosimetry, and eventually tested as adsorbents of methylene blue (MB) in aqueous solution.Yield is markedly higher with TR and similar with PET and VR, ranging between 40.1% and 11.1%. Using mixtures instead of the individual components in the preparation of CAs, significant mass changes occur, this proving that the starting materials interacted with each other during the preparation of CAs. In the case of PET and VR, it causes a substantial mass loss. As far as porosity is concerned, the trend is to an increase in macroporosity with VR, mesoporosity with TR and macro-, meso- and microporosity with mixed PET. Adsorption data for MB fit better to a pseudo-second-order kinetics than to a pseudo-first-order kinetics and to the Langmuir equation than to

the Freundlich equation. Adsorption is markedly faster and higher for CAs prepared from PET and VR containing mixtures. The simultaneous use of physically mixed various waste materials is a very simple method of preparing CAs with a controlled porous structure and adsorption behaviour.

Keywords: Rubber and plastic waste materials, steam activation, carbonaceous adsorbents, characterization, methylene blue adsorption.

_____

* Corresponding author: Fax: +34 924 271 149.

E-mail address: vgomez@unex.es (V. Gómez-Serrano).

1. Introduction

During the last decades, the consumption of polymers has increased steadily worldwide because of the population increase together with the trend of people to progressively improve their living conditions [1]. Polymeric materials of great commercial importance are rubbers and plastics. Rubber is largely used in the manufacture of vehicle tires (TR). From a plastic as polyethylene terephthalate (PET), specifically, synthetic fibers clothing (>60%) and plastic bottles (≈30%) are mainly produced [2]. Rubber/plastic ethylene propylene diene monomer (EPDM)/polypropylene (PP) blends (VR) have applications in household appliances, automobiles, buildings and constructions, and so on [3]. After end-of-life, TR, PET and VR are discarded and this results in the generation of large amounts of waste materials that, as rubbers and plastics are resistant against microbial attack [4,5], accumulate in environment and have a strong detrimental impact (e.g., plastics are the greatest thread for oceans and seas) and harmful effects on human health. The disposal of such amounts of waste materials represents a major environmental issue worldwide, mostly because

for the reduction of polymeric wastes the development of environmentally acceptable, that are further cost-effective, technologies is a difficult challenge due to complexities inherent in the reuse of polymers [6]. For this purpose, recycling was encouraged as the best alternative a few years ago [7-10]. TR, PET and VR may be valorised by conversion into value-added carbonaceous adsorbents (CAs) [11-13]. In fact, the development of CAs from scrap tires or PET has been studied before [14-21]. Here, using TR (rubber), PET (plastic) and VR (rubber/plastic) in systems of one, two and three components, CAs are prepared by thermal methods and characterized texturally as well as tested as adsorbents of methylene blue (MB) in aqueous solution. MB [7-(dimethylamino)phenothiazin-3-ylidene]-dimethylazanium chloride]), an organic cationic dye with chemical formula $C_{16}H_{18}N_3SCl.3H_2O$, was chosen as adsorptive because coloured organic effluents are produced in a number of industries including rubber and plastic. The discharge of dyes in the environment is a matter of growing concern for both toxicological and esthetical reasons [22]. Dyes can cause allergic dermatitis and skin irritation [23]. They can also have acute/or chronic effects on aquatic organisms, depending on their concentration and length of exposure [24]. Of MB is known its strong adsorption on solids [25], including carbons [26]. In fact, it is used as a test in the estimation of the properties of activated carbons [27], such as mesopores (20-30 Å) [28]. Also, MB often serves as a model compound for removing organic contaminants from aqueous solutions [25]. The overall objective of this study was to investigate the setting up of experimental methods for the simultaneous disposal and valorisation of rubber and plastic polymeric solid waste pollutants by preparation of porous materials with feasible applications in water purification treatments.

2. Materials and methods

75 *2.1. Raw materials*

76 As furnished kindly by Recipneu (Sines, Portugal), TR was made up of truck and
77 car rubbers in the ratio of 5:95. As received, TR was already wire-freed, shredded,
78 cryogenically size-reduced and sized, the fraction of particle sizes between 1 and 3 mm
79 being selected for subsequent studies. As a source of post consumed PET, bottles of
80 mineral water for human consumption were employed. VR was provided by Catelsa
81 Cáceres, S.A. Using scissors, PET and VR were progressively size-reduced until pieces
82 smaller than 5 mm were obtained. Data of the elemental analysis (C, H, N, S, $O_{diff.}$) and
83 proximate analysis (ash content) determined for TR, PET and VR are given in Table 1.

84 2.2. Carbonaceous adsorbents

85 2.2.1. Preparation

86 From each starting material separately and from mixtures of two and three
87 components at the mass ratio of 1:1 and 6:1:1, respectively, CAs were prepared by first
88 heating from ambient temperature to 900 ºC in N_2 or to 850 ºC in steam and by then
89 soaking at maximum heat treatment temperature (MHTT) for 2 h in horizontal
90 cylindrical electrical furnaces. The heating rate in both temperature ranges and
91 atmospheres was 10 ºC min^{-1}. For the steam activation experiments two furnaces placed
92 in series were used. One of them served as the steam generation system and the other
93 one as the activation system. The flow rate of liquid water (8 $mLmin^{-1}$) entering the
94 vapour generation system was controlled with a peristaltic pump and steam was carried
95 by a N_2 stream (flow rate = 100 $mLmin^{-1}$) to the activation system. The carbonization
96 and activation conditions used in the preparation of the CAs are summarized in Table 2,
97 which also lists yield values and sample codes.

98 2.2.2. Textural characterization

The textural characterization of the samples was carried out by N_2 adsorption at -196 ºC and by mercury porosimetry. Routinely, the samples were first oven-dried at 120 ºC overnight, allowed to cool down to room temperature in a $CaCl_2$ containing desiccator, and weighed. Then, the isotherms of gas adsorption were determined in a Quantachrome apparatus (Autosorb-1). Approximately, 10 mg of sample was placed in a glass holder and degassed at 250 ºC for 12 h, prior to adsorption. The experiments of mercury intrusion were performed in a Pore Master 60-Quantachrome porosimeter, using ~ 0.3 g of sample. Textural data obtained from the N_2 isotherms or from the curves of mercury intrusion are given in Table 3.

2.3. Adsorption of methylene blue

In the study of the adsorption process of MB (Panreac, reagent grade) experiments were carried out by the batch procedure, using a 10^{-3} mol L^{-1} aqueous solution. First, the UV-visible spectrum was recorded on a Shimadzu spectrophotometer (Model UV-1800) and from it the wavelength corresponding to the absorbance maximum at 664 nm was chosen. Second, it was checked that MB is stable in aqueous solution as a function of time (i.e., after more than 10 days had elapsed no colour and absorbance changes was observed in the MB solution) and also that Beer´s law is obeyed well for concentrations between 10^{-6}mol L^{-1} and $5x10^{-5}$mol L^{-1}. After that, either ≈ 0.10 g or between ≈ 0.002 and 0.30 g of adsorbent and 25 mL of MB solution were added to a suit of 25 mL test tubes, which were mounted at once in a Selecta (Unitronic-OR-C) thermostatic shaker bath with water at 25 ºC and an agitation of 50 oscillations min^{-1} and maintained under these conditions for 5 min-12 d or for an equilibration time, which was prefixed after previously carrying out kinetic experiments. Finally, the residual liquid was separated by filtration and eventually analysed at 664 nm. The adsorption of MB was quantified using the following mass balance equation:

$$q_e = (C_i - C_f)V/W \quad (1)$$

where q_e stands for the amount of MB adsorbed per unit weight of adsorbent, C_i and C_f are the initial and final concentrations of MB, V is the solution volume (L) and W is the adsorbent weight.

3. Results and discussion

3.1. Preparation of CAs. Process yield

The pyrolysis of rubbers and plastics entails the formation of a solid residue from the base polymer and from additives such as fillers, vulcanizing agents and activators, if used as compounding ingredients in their preparation. In connection with the chemical composition of such a residue, it was reported previously that for TR it has a high carbon content because of the important presence of carbon black in the rubber and also the main part of sulphur and zinc incorporated to the rubber (cross-linking and vulcanizing agents) [30]. For PET, the residue was a black glossy carbon of the equal size to the milled PET feed. The carbon has porous structure and was brittle but very hard [31]. With regard to the EPDM/PP (Santoprene) blend it was also detected the presence of a carbonaceous residue, representing approximately 10% of the initial weight of sample, after heating up to 550 ºC in a dynamic TG run [32], in spite of the fact that the thermal degradation of pure PP and EPDM separately at 550 or 700 ºC did not result in any char residue [32, 33]. In general, the amount of resulting residue depends on a number of factors such the number the starting material, reactor type, heating conditions and atmosphere. In Table 2 the yield values obtained in this study for the process of preparation of the samples are presented. As a guide, yield is 40.1% for T900, 24.1% for TS, 22.7 wt% for M7, and 20.4 wt% for M2. Therefore, as expected, yield is markedly higher when heating in steam because the mass loss in this

atmosphere occurred surely not only by pyrolysis as in N_2 but also by gasification processes. Furthermore, it can be observed that yield is higher with TR than with PET and VR and rather similar with PET and VR and also thereby when a mixture with a greater proportion of TR was used. The calculated average yield is 25.1% and ≈16.7% for all samples heated either in N_2 or in steam. As to the ≈16.7% yield it is also worth noting that this same value is obtained for the three sets of samples separately, i.e., for TS, PS and VS, M1-3 and M7-9. Of course, from these results it is apparent that the physically mixed starting materials did not interact with each other while being heated in the preparation of the samples. Nevertheless, some other factors with influence on the mass changes produced during the process of preparation of the sample may be at play here. Thus, yield is significantly lower for M3 than for PS and VS and also for M8 than for PS. In fact, as compared to the yields assessed from those obtained for TS, PS and VS by taking into account the mass used for each starting material, it is found that yield is substantially lower for M3 and M8, i.e., -16.7 and -12.2 %, respectively. Surprisingly, these results are compatible with the occurrence of chemical interaction between starting materials. If so, in view of the melting point of 147.0 ºC for PP, 144.7 ºC for EPDM/PP thermoplastic vulcanize [34] and 255 ºC for PET; TR polymers cannot melt because of cross-linking, it seems feasible that during heat treatment the EPDM/PP blend (i.e., EPDM particles closely dispersed in a PP matrix) melted at lower temperature and impregnated in part at least small PET pieces, making it possible the chemical interaction between components of initial mixtures. Furthermore, the impregnation and chemical processes could be promoted in the presence of a high content of PET (i.e., 50%, M3; 75%, M8) and under heating conditions above 255 ºC with both VR and PET in molten state. As a final comment it should be pointed out that for samples other than M3 and M8 the mass either increased for M2 (11.0%), M7

(6.11%) and M9 (4.3%) and slightly decreased for M1 (-1.07%).This almost negligible mass change indicates that TR and PET did not interact chemically when they were mixed together and heated in steam atmosphere.

3.2. Textural characterization of CAs

3.2.1. By N_2 adsorption at -196 ºC

The adsorption isotherms of N_2 measured for the CAs are shown in Figs.1 and 2. By their shape, in general, they are composite isotherms of types I or II and IV isotherms of the well-known BDDT classification system. These isotherm shapes have been associated in their turn with a micropore filling, monalayer-multilayer, and monolayer-multilayer-capillary condensation adsorption mechanism followed by adsorption systems made up of N_2(g) as adsorptive and microporous, non-porous, and mesoporous solids as adsorbents [35]. The derived values of S_{BET} and pore volumes, which are listed in Table 3, show that S_{BET} and W_0aresmall for T900 and V900 (i.e., V900 was non-amenable to the N_2-adsorption analysis) and that they increase slightly for TS, PS, VS, M2 and M9, more significantly for M1 and M7, and mostly for M3 and M8.Since $W_0$is 0.14 $cm^3\,g^{-1}$ for PS and 0.07 $cm^3\,g^{-1}$ for VS, on the one side, and 0.39 $cm^3\,g^{-1}$ for M3 and 0.34 $cm^3\,g^{-1}$ for M8, on the other side, it is evident that the use of PET and VR containing mixtures enhanced the development of microporosity, as compared to singly PET and VR. The effect on the porous texture of the samples must originate as a result of the mass loss produced during their preparation because of the presumable chemical interaction between VR and PET. However, W_0 is noticeably small not only for M8 than for M3, in spite of the fact that the PET content in the starting mixture was higher for M8 (75%) than for M3 (50 %), and therefore it appears that the beneficial effect on porosity was somehow mitigated by the presence of TR together with PET and VR in such a mixture. Accordingly, TR would dilute the action of VR on PET in respect of the

development of microporosity in the samples. In connection with V_{mi} and V_{me} it should be noted that V_{mi} is significantly smaller than W_0 and V_{me} is usually low for the CAs. Nevertheless, V_{me} is higher for TS (0.23 $cm^3 g^{-1}$), M1 (0.17 $cm^3 g^{-1}$) and M7 (0.20 $cm^3 g^{-1}$), which demonstrates the favourable influence of TR on mesoporosity of the samples.

3.2.2. By mercury porosimetry

Figs. 3 and 4 depict the graphical plots obtained from porosimetry data concerning the regions of meso- and mcropores of the samples. From these figures it follows that most of the CAs prepared in the present study are essentially macroporous materials, in particular V900, VS, M3 and M9 which are CAs with a predominant presence of pores with a radius between approximately 5000 and 250 Å.T900, TS, M1, M2 and M7, besides mainly macropores, also contain a significant fraction of wide mesopores with pore radii of ≈250-150 Å. Not only for TS but also for P900, PS, M1,M3 and M8 the mesopore-size distribution is even wider, embracing pores of varying radius in the range of 150-20 Å. According to the slope of the curves of mercury intrusion, TS is the CA that possesses the most heterogeneous porosity in the regions of macro- and mesopores. It is also worth noting that, of all samples prepared in the present study, M3 is the only CA with a higher content of different size narrowest mesopores. In brief, from these results it becomes apparent that the general trend is to an increased content of meso- and macropores with TR, macropores with VR and thereby meso- and macropores with PET containing mixtures. Notice that meso-and macroporosity are very poorly developed in P900 and PS. The values of pore volumes collected in Table 3 show first that the highest values of $V_{me\text{-}p}$ are by far 0.35 $cm^3 g^{-1}$ for T900, 0.32 $cm^3 g^{-1}$ for TS and 0.31 $cm^3 g^{-1}$ for M7. Furthermore, $V_{ma\text{-}p}$ is 1.24 $cm^3 g^{-1}$ for VS and 1.26 $cm^3 g^{-1}$ for M9. For T900 and TS $V_{ma\text{-}p}$ is 0.37 and 0.73 $cm^3 g^{-1}$, respectively; i.e., also high, though much less than for V900 and VS. Secondly, $V_{me\text{-}p}$ is 0.02 $cm^3 g^{-1}$ for PS and 0.31 $cm^3 g^{-1}$ for

M7. Likewise, V_{ma-p} is 0.02 $cm^3 g^{-1}$ for PS and as high as 1.06 $cm^3 g^{-1}$ for M3. On the other hand, as expected in view of the V_{ma-p} values and estimate method, V_T is 1.32 $cm^3 g^{-1}$ for VS, 1.69 $cm^3 g^{-1}$ for M3 and 1.51 $cm^3 g^{-1}$ for M9, and therefore also higher for CAs prepared using VR alone and mixed with other starting materials.

The values of V_{me-p} and V_{ma-p} in Table 3 provide further valuable insight into the influence on meso- and macroporosity of the starting material/mixture and the method used in the preparation of the samples. Thus, the somewhat higher V_{me-p} for T900 than for TS reveals that mesopores largely originated as a result of the pyrolysis of TR, whereas the macropores should arise from the partial gasification of VR and TR in steam atmosphere. The chemical interaction between PET and VR should result in a significant development of mesoporosity, as proved especially by the values of V_{me-p} obtained for M3 and M8-9 as compared to those for PS and VS. As far as macroporosity is concerned, the only somewhat lower V_{ma-p} for M3 (1.06 $cm^3 g^{-1}$) than for VS (1.24 $cm^3 g^{-1}$) together with the very small V_{ma-p} for P900 (0.04 $cm^3 g^{-1}$) and PS (0.02 $cm^3 g^{-1}$) argues for a favourable influence of the chemical interaction between VR and PET on the creation of macropores. It is further consistent with the very high V_{ma-p} for M9 (1.26 $cm^3 g^{-1}$). By contrast, the values of V_{ma-p} for M1 (0.35 $cm^3 g^{-1}$) and M2 (0.66 $cm^3 g^{-1}$) point out that TR and PET did not interacted with each other and that in the case of TR and VR the interaction unfavourably influenced macroporosity. However, the opposite applies to VR as long as it was in a large excess with respect to TR and PET in the starting mixture, as in the preparation ofM9. Finally, it should be mentioned that for a larger number of samples V_{me-p} is higher than V_{me}, which is in line with the application of controlled external pressure for mercury intrusion in pores of a porous solid dispersed in mercury.

3.2.3. Comparison of textural properties

Comparison of the apparent surface area and pore volumes for CAs with those obtained previously for CAs prepared from TR and PET separately by steam activation as well (see Table 4, [36-56]) (i.e., as far as to our knowledge, EPDM/PP has not been used before in the preparation of CAs) reveals that they are frequently similar. Textural property discrepancies depending on the source as rule can be accounted for if one takes into account that the preparation of CAs by steam activation is greatly influenced not only by the starting material but also by the steam flow and heating conditions, as illustrated by the S_{BET} values obtained previously for PET-derived CAs, which vary in the ranges of 705-1215 m^2 g^{-1} with steam flows of 1.95-11.6 mL min^{-1} and of 4-1235 m^2 g^{-1} and 1163-1202 m^2 g^{-1} by heat-treating at 600-900 ºC and for 0.25-2 h, respectively [56]. Furthermore, the development of porosity was also likely influenced by the method of a single heat treatment in steam used in the preparation of CAs, because of the simultaneous thermal degradation (pyrolysis) and activation processes of the starting materials. Moreover, it should be pointed out that such a method has economic advantages over the usual method of two successive carbonization and activation stages.

3.3. Adsorption process of MB

3.3.1. Adsorption kinetics

The data of concentration of the MB solution (C) as a function of time (t) obtained in the study of the adsorption kinetics of MB on the CAs are plotted in Figs. 5 and 6. At a simple glance, from these figures it follows that kinetics as a rule was faster with the CAs prepared from mixed components than from the single ones. The kinetic data were fitted to the pseudo-first order rate equation of Lagergren [57] and to the pseudo-second order rate equation of Ho and Mckay [58]. The former rearranged to a linear form is usually written as:

$$log(q_e - q_t) = logq_e - \frac{K_1}{2.303}t \quad (2)$$

with q_e and q_e being the adsorption capacities at equilibrium and at time t, respectively, and $k_1$is the rate constant of first order adsorption. Therefore, the plot of log (q_e – q_t) versus t should be a straight line with slope log q_e and intercept –k_1/2.303.

By assuming that the adsorption capacity is proportional to the number of active sites occupied on the surface of the adsorbent, the Ho and Mckay equation [58] in the integrated rate law for the pseudo-second order reaction is:

$$\frac{t}{q_t} = \frac{1}{K_2 q_e^2} + \frac{1}{q_e}t \quad (3)$$

$$\text{with } h = k_2 q_e^2 \quad (4)$$

where q_e and q_t are the amounts of MB adsorbed on the surface of the adsorbent at equilibrium and at any time t, respectively, and k_2 is the rate constant of second order adsorption and h is the initial adsorption rate. Here, the plot of t/q_t against t should give a linear relationship, from which q_e and k_2 can be obtained.

The equilibration time (t_e, h) together with the values of q_e, $k_{1,2}$ and R^2 obtained for the various CAs-BM adsorption systems by using equations (2) and (3) are given in Table 5. First, it is worth noting that t_e varies in the wide range of 12-168 h. The t_e values indicate that the kinetics of the overall adsorption process is faster by the order P900 = V900 > M3 >> M2 >> the rest of CAs. On the other, from the R^2 values it becomes clear that the kinetic data fit better to the pseudo second order adsorption than to the pseudo first order adsorption. Furthermore, k_2 (g mol^{-1} h^{-1}) varies by P900 > V900 >>M3 > other samples. The so fast kinetics with P900 and V900, the adsorption to a large extent being almost an instantaneous process, can be accounted for by the majority presence of large size pores in these CAs (see data in Table 5), which would

make easy the access of MB to surface adsorption sites. In the case of M3, which is a CA possessing well developed porosity in the regions of not only meso- and macropores but also micropores (see Figs. 2 and 4 and Table 3), it is likely however that the diffusion of such a large size adsorptive as the BM molecule was somehow hindered, this decelerating the adsorption process. In this connection it is worth mentioning that the in dilute solution in water MB is present mostly as a monomer, the approximate molecular dimensions being 12.5 to 16.0 Å long by 5.7 to 8.4 Å wide with a thickness of about 5 Å [59], 13.82 Å in length and with 5.91 Å wide [60], and 17.0 x 7.6 x 3.3 Å[61]. Therefore, it can be foreseen that the fact that MB is a long tridimensional molecule was the main factor with influence on its diffusion in micropores of the adsorbent. The adsorption in micropores with M3 as the adsorbent is further proved by the high q_e (1.96 x 10^{-4} mol g^{-1}) obtained for this sample, as in micropore walls concentrates most surface area of porous solids. It also applies to PS, M7 and M8, which as a rule are CAs with high W_0. By contrast to P900, V900 and M3, k_2 is markedly smaller for M1, T900, M2 and TS, all these samples having been prepared from TS. In brief, it may be stated that by using the stating materials separately or mixed with each other in the preparation of CAs, the kinetics of the adsorption process of MB in aqueous solution is faster and slower for the CAs prepared with PET and VS and with TR, respectively.

3.3.2. Adsorption isotherms

The isotherms measured for the adsorption of MB in aqueous solution on the CAs are plotted in Figs. 7 and 8. According to the system of classification of solution adsorption isotherms for organic solutes put forward by Giles et al. [62] more than fifty years ago, the aforesaid isotherms belong to the class L, which is the normal or "Langmuir" isotherm, usually indicative of molecules adsorbed flat on adsorbent

surface. A flat, rather than end-on, MB adsorption in micropores is compatible with the big size of the MB, which is 12.5-17.0 Å long [59, 61], and therefore not too much shorter than the greater microropore width of 20 Å. Accordingly, because of steric hindrance, the MB could adopt a flat orientation on adsorbent surface. The occurrence of π-πdispersive interactions between aromatic rings of the MB molecule and adsorbent surface, as reported in previous studies [60 and refs. therein], could also contribute to the flat adsorption of the MB molecule. For that, as MB is a 17.0 x 7.6 x 3.3 Å three dimensional molecule [61], it would be necessary that MB suffered structural distortion, perhaps involving the dimethylamino groups because of their supposedly distorted trigonal pyramidal geometrical shape. The reported projected area of the MB molecule ranges between 130-135 Å [61]. On the other hand, the adsorption isotherms obtained for the CAs-MB systems as a rule display a marked adsorption rise up to $C/C_0 \approx 0.1$ and a long plateau above this C/C_0. The former isotherm feature argues for a high affinity of MB for the adsorbent. The latter feature means that a high energy barrier has to be overcome before additional adsorption can occur on new sites, after the surface has been saturated to the first degree. Also, the solute has high affinity for the solvent, but low affinity for the layer of solute molecules already adsorbed [62] Furthermore, the isotherms of T900 (Fig. 1) and M1 show a significant adsorption increase beyond the plateau, at C/C_0 above about ≥ 0.6, which was connected previously with the adsorption on a fresh surface, i.e., the exposed parts of the layer already present, new surface or part of the original surface [62].

The adsorption of MB under equilibrium conditions was analysed by the Langmuir isotherm that in the linear form is:

$$\frac{C_e}{q_e} = \frac{1}{Q_0 b} + \frac{C_e}{Q_0} \qquad (5)$$

here q_e is the specific adsorption of MB, C_e is the equilibrium concentration, Q^0 is the monolayer adsorption capacity and b is the constant related to free energy or net enthalpy of adsorption ($b \propto e^{-\Delta H/RT}$). In Table 6 the values of Q^0 and b obtained from the slope and intercept of the plots of $C_e/q_e = f(C_e)$ are presented.

The Freundlich equation was also used:

$$logq_e = logK_F + \frac{1}{n} logC_e \quad (6)$$

where K_f and n are the Freundlich constants which correspond to adsorption capacity and adsorption intensity, respectively. Therefore, the plots of log q_e against log C_e should therefore be a straight line with slope log K_F and intercept 1/n. The resulting values of K_F and 1/n for the CAs-MB adsorption systems under study are given in Table 6. The n value indicates the degree of nonlinearity between solution concentration and adsorption, as follows: if n = 1, then adsorption is linear; if n < 1, then adsorption is a chemical process; if n > 1, then adsorption is a physical process. Since the values of n obtained here, which are omitted for the sake of brevity, are in the range 0.02-10, it indicates physical adsorption of MB on the CAs. It further represents good BM adsorption [63 and ref. therein].

From the values of R^2 listed in Table 6 it follows that the equilibrium experimental data as a rule fit very well to the Langmuir equation (i.e., R^2 is higher than 0.990 for a large number of adsorption systems) and considerably better to such an equation than to the Freundlich equation. Furthermore, Q^0 (mol L^{-1}) varies in the range between 0.00 for P900 and 0.92 10^{-3} for M8. Q^0 is also as high as 0.85 x 10^{-3} mol L^{-1} for M3. Therefore, the higher Q^0 values for these two CAs, which were prepared from PET and VS containing mixtures, are consistent with the larger degree of microporosity development in this couple of samples. For comparison purposes it is interesting to point out that Q^0

368 is = 0.72 x 10^{-3} for PS and 0.52 x 10^{-3} for VS and from these results it becomes also
369 evident therefore that the use of mixed PET and VR, both together and also with TR,
370 benefits the adsorption process of MB from the equilibrium standpoint. The favorable
371 influence on adsorption was greater as the content of PET in the starting mixture
372 increased, which was 75 % for M9, 50% for M3, 12.5 % M9 (Q^0, 0.50 x 10^{-3}) and 0.0%
373 for M2 (Q^0, 0.42 x 10^{-3}).

374 **4. Conclusions**

375 From the above results, it may be concluded that the use of TR, PET and VR mixed
376 with each other rather than separately in the preparation of CAs by heat treatment at
377 high temperature in N_2 or steam atmosphere entails the interaction between starting
378 materials, as evidenced not only from mass changes but also by textural effects and
379 behaviour of CAs in the adsorption of MB in aqueous solution. The mass of sample
380 either increases or decreases depending on whether TR or VR is a main component of
381 the starting mixture. At most, it is +11.0 % for M2 and -16.7 % for M3. Regarding
382 porosity, the general trend is to an increase in macroporosity with VR, mesoporosity
383 with TR, and macro-, meso- and microporosity with mixed PET. For M3 (i.e., the CA
384 prepared from the 1:1 PET and VR mixture) S_{BET} is 675 $m^2\,g^{-1}$ and the micro-, meso-,
385 macro- and total pore volumes are 0.39, 0.15, 1.06 and 1.60 $cm^3\,g^{-1}$, whereas for PS (i.e.,
386 the CA prepared using PET only) S_{BET} is 248 $m^2\,g^{-1}$ and the pore volumes are in turn
387 0.14, 0.02, 0.02 and 0.18 $cm^3\,g^{-1}$. M3 is the only CA with a higher content of different
388 size narrowest mesopores. Adsorption data obtained for MB fit better to a pseudo-
389 second-order kinetics than to a pseudo-first-order kinetics and to the Langmuir equation
390 than to the Freundlich equation. Adsorption is markedly faster for CAs prepared from
391 PET and VR containing mixtures. The adsorption capacity was larger with the increase
392 of the PET content in the starting mixture. The simultaneous use of physically mixed

various waste materials is a very simple method to prepare ACs with tailored properties and behaviours, simply by controlling the composition of the starting heterogeneous mixture.

Acknowledgments

Financial support from the Spanish Ministerio de Ciencia e Innovación through project CTM2008-03636 and from the Junta de Extremadura and European Funds for Regional Development (ERDF) through the aid to Research Groups (GR18013) is gratefully acknowledged.

References

[1] Hamad, K., Kaseem, M., Deri, F.: Recycling of waste from polymer materials: An overview of the recent works. Polym. Degrad. Stab. 98, 2801-2812 (2013).

[2] Ji, L.N.: Study on preparation process and properties of polyethylene terephthalate (PET). Appl. Mech. and Mater.312, 406–410 (2013).

[3] Naskar, K., Gohs, U., Wagenknecht, U., Heinrich, G.: PP-EPDM thermoplastic vulcanisates (TPVs) by electron induced reactive processing. eXPRESS Polym. Lett. 3, 677-683 (2009).

[4] Shah, A.A., Hasan, F., Shah, Z., Kanwal, N., Zeb, S.: Biodegradation of natural and synthetic rubbers: a review. Int. Biodeter. Biodegr. 83, 145-157 (2013).

[5] Shah, A.A., Hasan, F., Hameed, A., Ahmed, S.: Biological degradation of plastics: A comprehensive review. Biotechnol. Adv. 26, 246-265 (2008).

[6] Burillo, G., Clough, R.L., Czvikovszky, T., Guven, O., Le Moel, A., Liu, W., Singh, A., Yang, J.,Zaharescu, T.: Polymer recycling: potential application of radiation technology. Radit. Phys. and Chem. 64, 41-51 (2002).

416 [7] Stevenson, K., Stallwood, B., Hart, A.G.: Tire rubber recycling and bioremediation:
417 a review. Bioremediat. J. 12, 1-12 (2008).
418 [8] Al-Salem, S.M., Lettieri, P., Baeyens, J.: Recycling and recovery routes of plastic
419 solid waste (PSW): a review. Waste Manage. 29, 2625-2643 (2009).
420 [9] Ramos, G., Aguacil, F.J., López, F.A.: The recycling of end-of-life tyres.
421 Technological review. Rev. Met. 47, 273-284 (2011).
422 [10] Yazdi, M.A., Yang, J., Yihui, L., Su, H.: A review on application of waste tire in
423 concrete. Int. J. of Civ., Environ., Struct., Const. and Archit. Eng. 9, 1648-1661 (2015).
424 [11] Bazargan, A., Hui, C.W., Mckay, G.: Porous carbons from plastic waste. Adv.
425 Polym. Sci. 266, 1-26 (2015).
426 [12] Wójtowicz, M.A, Serio, M.A: Pyrolysis of scrap tires: can it be profitable?.
427 Chemtech. 26, 48-53 (1996).
428 [13] Dias, J.M., Alvim-Ferraz, M.C.M., Almeida, M.F., Rivera-Utrilla, J., Sánchez-
429 Polo, M.: Waste materials for activated carbon preparation and its use in aqueous-phase
430 treatment: a review. J. Environ. Manage. 85, 833-846 (2007).
431 [14] Lehmann, C.M.B., Rostam-Abadi, M.Rood, M.J., Sun,J.: Reprocessing and reuse
432 of waste tire rubber to solve air-quality related problems. Energy Fuels 12, 1095-1099
433 (1998).
434 [15] López, F.A., Centeno, T.A., Aguacil, F.J.,Lobato, B., López-Delgado, A., Fermoso,
435 J.: Gasification of the char derived from distillation of granulated scrap tyres. Waste
436 Manage. 32, 743-752 (2012).
437 [16] Heras, F., Alonso, N., Gilarranz, M.A, Rodríguez, J.J.: Activation of waste tire char
438 upon cyclic oxygen chemisorption-desorption. Ind. Eng. Chem. Res. 48, 4664-4670
439 (2009).

440 [17] Manchón-Vizuete, E.,Macías-García, A., Nadal Gisbert, A., Fernández-González,
441 C., Gómez-Serrano, V.: Preparation of mesoporous and macroporous materials from
442 rubber of tyre wastes. Microporous Mesoporous Mat. 67, 35-41 (2004).
443 [18] Parra, J.B., Ania, C.O., Arenillas, A., Rubiera, F., Pis, J.J.: High value carbon
444 materials from PET recycling. Appl. Surf. Sci. 238, 304-308 (2004).
445 [19] Fernández-Morales, I., Almazán-Almazán, M.C., Pérez-Mendoza, M., Domingo-
446 García, M.,López-Garzón, F.J.: PET as precursor of microporous carbons: preparation
447 and characterization. Microporous Mesoporous Mat 80, 107-115 (2005).
448 [20] A. Esfandiari, A., Kaghzchi, T., Soleimani, M.: Preparation and evaluation of
449 activated carbons obtained by physical activation of polyethyleneterephthalate (PET)
450 wastes. J. Taiwan Inst. Chem. E. 43, 631-637 (2012).

451 [21] Bratek, W., Swiatkowski, A., Pakula, M.,Biniak, S., Bystrzejewski,
452 M.,Szmigielski, R.: Characteristics of activated carbon prepared from waste PET by
453 carbon dioxide activation. J. Anal. Appl. Pyrolysis 100, 192-198 (2013).

454 [22] Rafatullah, M.,Sulaiman, O.,Hashim, R., Ahnada, A.: Adsorption of methylene
455 blue on low-cost adsorbents: A review. J. Hazard. Mater. 177, 70-80 (2010).

456 [23] Lorenc-Grabowska, E., Gryglewicz, G.: Adsorption characteristics of Congo Red
457 on coal-based mesoporous activated carbon. Dyes Pigm. 74, 34-40 (2007).

458 [24] Pereira, L., Alves, M.: Dyes–Environmental impact and remediation. In: Malik, A.,
459 Grohamann, E. (eds.) Environmental Protection Strategies for Sustainable
460 Development, pp. 111-162, Springer, Dordrecht (2012).

461 [25] Salman,J.M.: Preparation of mesoporous-activated carbon from branches of
462 pomegranate trees: Optimization on removal of methylene blue using response surface
463 methodology. J. Chem. (2013). doi: 10.1155/2013/489670.

[26] Kannan, N., Sundaram, M.M.: Kinetics and mechanism of removal of methylene blue by adsorption on various carbons-a comparative study. Dyes Pigm. 51, 25-40 (2001).

[27] Jankowska, H., Swiatkowski, A., J. Choma, J.: Active Carbon. Ellis Horwood, New York (1991).

[28] Adibfar, M., Kaghazchi, T., Asasian, N., Soleimani, M.: Conversion of poly(ethylene terephthalate) waste into activated carbon: chemical activation and characterization. Chem. Eng. Technol. 37, 979-986 (2014).

[29] Dubinin, M.M.: Physical adsorption of gases and vapors in micropores. In: Cadenhead, D.A., Danielli, J.F., Rosenberg, M.D. (eds.) Progress in Surface and Membrane Science, pp. 1-70, Academic Press, New York (1975).

[30] Bouvier, J.M.,Clin, F.: Pyrolysis of rubber and tyres waste. Commission des Communautés Européennes, Report du B.R.G.M.: 85DAM 029 MIN, pp. 1-91 (1985)

[31] Brems, A., Baeyens, J., Vandecasteele, C., Dewil, R.: Polymeric cracking of waste polyethylene terephthalate to chemicals and energy. J. Air & Waste Manage. Assoc. 61, 721-731 (2011).

[32] Navarro, R., Torre, L., Kenny, J.M., Jiménez, A.: Thermal degradation of recycled polypropylene toughened with elastomers, Polym. Degrad. Stab. 82, 279-290 (2003).

[33] Tang, G., Hu, Y., Song, L.: Study on the flammability and thermal degradation of a novel intumescent flame retardant EPDM composite. Procedia Eng. 62, 371-376 (2013)

[34] Brostow W., Datashvili T., Geodakyan J., Lou J.: Thermal and mechanical properties of EPDM/PP + thermal shock-resistant ceramic composites. J. Mater. Sci. 46, 2445-2455 (2011).

[35] Gregg, S.J., Sing, K.S.W.: Adsorption, Surface Area and Porosity. Academic Press, London (1982).

[36] Ogasawara, S., Kuroda, M., Wakao, N.: Preparation of activated carbon by thermal decomposition of used automotive tires. Ind. Eng. Chem. Res. 26, 2552-2556 (1987).

[37] Sun, J., Brady, T.A., Rood, M.J., Lehmann, C.M.: Adsorbed natural gas storage with activated carbons made from Illinois coals and scrap tires. Energy Fuels 11, 316-322 (1997).

[38] Cunliffe, A.M., Williams, P.T.: Influence of process conditions on the rate of activation of chars derived from pyrolysis of used tires. Energy Fuels 13, 166-175 (1999).

[39] Helleur, R., Popovic, N., Ikura, N., Stanciulescu, M., Liu, D.: Characterization and potential applications of pyrolytic char from ablative pyrolysis of used tires. J. Anal. Appl. Pyrolysis 58-59, 813-824 (2001).

[40] Lin, Y.-R., Teng, H.: Mesoporous carbons from waste tire char and their application in wastewater discoloration. Microporous Mesoporous Mat. 54, 167-174 (2002).

[41] Ariyadejwanich, P., Tanthapanichakoon, W., Nakagawa, K., Mukai, S.R, Tamon, H.: Preparation and characterization of mesoporous activated carbon from waste tires. Carbon 41, 157-164 (2003).

[42] Nakagawa, K., Namba, A., Mukai, S.R., Tamon, H., Ariyadejwanich, P., Tanthapanichakoon, W.: Adsorption of phenol and reactive dye from aqueous solution on activated carbons derived from solid wastes. Water Res. 38, 1791-1798 (2004).

[43] Zabaniotou, A., Madau, P., Oudenne, P.D., Jung, C.G., Delplancke, M.P., Fontana, A.: Active carbon production from used tire in two-stage procedure: industrial pyrolysis

511 and bench scale activation with H_2O-CO_2 mixture. J. Anal. Appl. Pyrolysis 72, 289-297
512 (2004).
513 [44] Tanthapanichakoon, W., Ariyadejwanich, P., Japthong, P., Nakagawa, K., Mukai,
514 S.R., Tamon, H.: Adsorption-desorption characteristics of phenol and reactive dyes
515 from aqueous solution on mesoporous activated carbon prepared from waste tires.
516 Water Res. 39, 1347-1353 (2005).
517 [45] López, G., Olazar, M., Artetxe, M., Amutio, M., Elodi, G., Bilbao, J.: Steam
518 activation of pyrolytic tyre char at different temperatures. J. Anal. Appl. Pyrolysis 85,
519 539-543 (2009).
520 [46] González, J.F., Encinar, J.M., González-García, C., Sabio, E., Ramiro, A., Canito,
521 J.L., Gañan, J.: Preparation of activated carbons from used tyres by gasification with
522 steam and carbon dioxide. Appl. Surf. Sci. 252, 5999-6004 (2006).
523 [47] Galvagno, S., Casciaro, G., Casu, S., Martino, M., Mingazzini, C., Russo, A.,
524 Portofino,S.: Steam gasification of tyre waste, poplar, and refuse-derived fuel: a
525 comparative analysis. Waste Manage. 29, 678-689 (2009).
526 [48] Bóta, A., László, K., Nagy, L.G., Copytzky, T.: Comparative study of activated
527 carbons from different precursors. Langmuir 13, 6502-6509 (1997).
528 [49] László, K., Bóta, A., Nagy, L.G., Cabasso, I.: Porous carbon from polymer waste
529 materials. Colloids Surf. A 151, 311-320 (1999).
530 [50] László, K.: Adsorption from aqueous phenol and aniline solutions on activated
531 carbons with different surface chemistry. Colloids Surf. A 26, 32-39 (2005).
532 [51] László, K., Podkoscielny, P., Dabrowski, A.: Heterogeneity of activated carbons
533 with different surface chemistry in adsorption of phenol from aqueous solutions. Appl.
534 Surf. Sci. 252, 5752-5762 (2006).

[52] Marzec, M., Tryba, B., Kalenczuk, R.J., Morawski, A.W.: Poly(ethylene terephthalate) as a source for activated carbon. Polym.Adva. Technol. 10, 588-595 (1999).

[53] Tamon, H., Nakagawa, K., Suzuki, T., Nagano, S.: Improvement of mesoporosity of activated carbon by novel pretreatment for steam activation. Carbon 37, 1643-1645 (1999).

[54] Nakagawa, K., Mukai, S.R., Suzuki, T., Tamon, H.: Gas adsorption on activated carbons from PET mixtures with metal salt. Carbon 41, 823-831 (2003).

[55] Sych, N.V., Kartel, N.T., Tsybs, N.N., Strelko, V.V.: Effect of combined activation on the preparation of high porous active carbons from granulated post–consumer polyethyleneterephthalate. Appl. Surf. Sci. 252, 8062-8066 (2006).

[56] Mendoza-Carrasco, R., Cuerda-Correa, E.M., Alexandre-Franco, M.F., Fernández-González, C., Gómez-Serrano, V.: Preparation of high-quality activated carbon from polyethyleneterephthalate (PET) bottle waste. Its use in the removal of pollutans in aqueous solution. J. Environ. Manage. 181, 522-535 (2016).

[57] Lagergren, S.; About the theory so-called adsorption of soluble substances, Kungliga Svenska Vetenskapsakademiens Handlingar 24, 1-39 (1898).

[58] Ho, Y.-S., McKay, G.; Pseudo-second order model for sorption processes. Process. Biochem. 34, 451-465 (1999).

[59] Grattan-Bellew, P.E.: Petrographic and technological methods for evaluation of concrete aggregates. In: Ramachandran, V.S., Beaudoin, J.J. (eds.) Handbook of Analytical Techniques in Concrete Science and Technology: Principles, Techniques, and Applications, pp. 63-104. Noyes Publications, Park Ridge, NJ (2001).

[60] de SouzaMacedo, J., Bezerra da Costa Júnior, N., Almeida, L.E., Fragoso da Silva Vieira, E., Cestari, A.R., Gimenez, L. de F., Villarreal Carreño, N.L., Silva Barreto, L.:

Kinetic and calorimetric study of the adsorption of dyes on mesoporous activated carbon prepared from coconut coir dust. J. Colloid Interface Sci. 298, 315-322 (2006).

[61] Arias, M., López, E., Nuñez, A., Rubinos, D., Soto, B., Barral, M.T., Díaz-Fierros, F.: Adsorption of methylene blue by red mud, an oxide-rich byproduct of bauxite refining. In: Berthelin, J., Huang, P.M., Bollag, J.M., Andreux, F. (eds.) Effect of Mineral-Organic-Microorganism Interactions on Soil and Freshwater Environments, pp. 361-365, Springer, Boston, MA (1999).

[62] Giles, C.H., MacEwan, T.H., Nakhwa, S.N., Smith, D.: Studies in adsorption. Part XI. A system of classification of solution adsorption isotherms, and its use in diagnosis of adsorption mechanisms and in measurement of specific surface areas of solids. J. Chem. Soc, London 111, 3973-3993 (1960).

[63] Berhe Desta, M.: Batch sorption experiments: Langmuir and Freundlichisothem studies for the adsorption of textile metal ions onto teff straw (Eragrostistef) agricultural waste. J. Thermodynamics (2013). doi: 10.1155/2013/375830.

Table headings

Table 1. Data of chemical analyses of the starting materials

Table 2. Preparation of CAs. Yield and notations

Table 3. Textural data of CAs

Table 4. Preparation of activated carbon from tire rubber and PET wastes. Results of steam activation from the literature.

Table 5. Adsorption kinetic of MB

Table 6. Adsorption isotherms of MB

Captions to figures

Fig. 1 Adsorption isotherms of N_2 at -196 ºC for the CAs prepared from TR, PET and VR separately

Fig. 2 Adsorption isotherms of N_2 at -196 ºC for the CAs prepared from two and three component mixtures

Fig. 3 Curves of mercury intrusion for the CAs prepared from TR, PET and VR separately

Fig. 4 Curves of mercury intrusion for the CAs prepared from two and three component mixtures

Fig. 5 Adsorption kinetics of MB on CAs prepared from single waste materials

Fig. 6 Adsorption kinetics of MB on CAs prepared from mixed waste materials

Fig. 7 Adsorption isotherms of MB on CAs prepared from single waste materials

Fig. 8 Adsorption isotherms of MB on CAs prepared from mixed waste materials

Table 1

Chemical analyses of TR, PET and VR (wt%).

Material	C	H	N	S	$O_{diff.}$	Ashes
TR	85.1	7.41	0.33	1.81	5.4	7.10
PET	62.9	4.27	0.00	0.00	32.8	0.00
VR	88.0	11.82	0.00	0.37	0.00	0.93

608

609 **Table 2**

610 Preparation of CAs. Yield and notations.

Starting material/mixture	Ratio	Atmosphere	MHTT/ ºC	Soaking time/h	Yield/ wt%	Code
TR		N_2	900	2	40.1	T900
PET		N_2	900	2	17.1	P900
VR		N_2	900	2	18.1	V900
TR		H_2O(v)	850	2	24.1	TS
PET		H_2O(v)	850	2	13.7	PS
VR		H_2O(v)	850	2	12.2	VS
TR/PET	1:1	H_2O(v)	850	2	18.7	M1
TR/VR	1:1	H_2O(v)	850	2	20.4	M2
PET/VR	1:1	H_2O(v)	850	2	11.1	M3
TR/PET/VR	6:1:1	H_2O(v)	850	2	22.7	M7
PET/TR/VR	6:1:1	H_2O(v)	850	2	13.2	M8
VR/TR/PET	6:1:1	H_2O(v)	850	2	14.5	M9

611

612

Table 3

Textural data of CAs.

Sample	S_{BET}[a]/ $m^2\,g^{-1}$	W_0[a]/ $cm^3\,g^{-1}$	V_{mi}[a]/ $cm^3\,g^{-1}$	V_{me}[a]/ $cm^3\,g^{-1}$	$V_{me\text{-}p}$[b]/ cm^3g^{-1}	$V_{ma\text{-}p}$[b]/ $cm^3\,g^{-1}$	V_T[a,b]/ $cm^3\,g^{-1}$
T900	64	0.05	0.01	0.04	0.35	0.37	0.77
P900	0.0	0.00	0.00	0.00	0.07	0.04	0.11
V900	28	0.02	0.01	0.07	0.05	0.70	0.77
TS	278	0.19	0.13	0.23	0.32	0.73	1.24
PS	248	0.14	0.03	0.12	0.02	0.02	0.18
VS	100	0.07	0.08	0.04	0.01	1.24	1.32
M1	353	0.22	0.17	0.17	0.18	0.35	0.75
M2	153	0.11	0.07	0.13	0.19	0.66	0.96
M3	675	0.39	0.33	0.13	0.15	1.06	1.60
M7	358	0.23	0.17	0.20	0.31	0.81	1.35
M8	572	0.34	0.28	0.16	0.18	0.41	0.93
M9	264	0.17	0.12	0.12	0.08	1.26	1.51

[a]The N_2 adsorption isotherm; S_{BET}, BET surface area (p/p^0 = 0.05-0.30, am = 16.2 Å^2); W_0micropore volume (Dubinin-Radushkevich equation [29]); V_{mi}, micropore volume (V_{ad} at p/p^o = 0.10, V_{ad} = volume adsorbed); V_{me} , mesopore volume (V_{ad} at p/p^o = 0.95 at p/p^o = 0.10). W_0, V_{mi} and V_{me} are expressed as liquid volumes. [b] Mercury porosimetry: $V_{me\text{-}p}$, mesopore volume; $V_{ma\text{-}p}$ macroporore volume. $V_T = W_0 + V_{me\text{-}p} + V_{ma\text{-}p}$.

624 **Table 4**

625 Preparation of activated carbon from tire rubber and PET wastes. Results of steam
626 activation from the literature.

Starting material	Charring conditions (ºC, h, atm.)	Activation conditions (ºC, h)	Yield/ wt%	S_{BET}/ $m^2\ g^{-1}$	Volume of micropores /$cm^3\ g^{-1}$	Volume of mesopores /$cm^3\ g^{-1}$	References
Tire rubber		700-900, 3	9	1260			[36]
	600, 0.75, N_2	850-900, 1-3		420-1031	0.13-0.28		[37]
	450, 90, N_2	935, 0.5-11.5	35	640			[38]
	600, 4, N_2	900, 1-3	84-74	254, 272			[39]
		900		238-602	22%	78%	[40]
	500, 1, N_2	850	68-24	386-755	0.12-0.26	0.21-1.09	[41]
	500, 1, N_2	850, 0.5-1.5		770	0.30	0.66	[42]
	800, 0.75, N_2	970, 2-2.5	40-35	432			[43]
	500, N_2	850	35	985	0.37	0.79	[44]
	500, N_2	850, 900		>500			[45]
	1, 800, N_2	750-900, 1-3	91-13	85-1317	0.03-0.47	0.19-1.25	[46]
		1000, 3	9.5	548			[47]
PET	700 or 750, N_2	900, 1.5	50	1190-1443	0.42-0.65		[48-51]
	500, 2, N_2	500	17.1	359			[52]

500, N_2	850, 0.5-4	22	1700	0.93	0.15	[53]
500, 1, N_2	850, 0.08-4	88-22	394-1740	0.21-0.93	0.04 -0.15	[54]
500, 1, N_2	850, 0.5, 1.5		1200	0.55	0.21	[42]
H_2SO_4, 1-24	500-800, ≈0.05-0.5	≈ 15	1030	0.36		[55]
	600-900, 1	≈17-8	4-1235	0-0.74	0-0.35	[56]

627

628

629 **Table 5**

Sample	t_e/h	pseudo-first-ordermodel			pseudo-second-ordermodel		
		$q_e \cdot 10^4$/ mol g^{-1}·	$k_1 \cdot 10^3$/ h^{-1}	R^2	$q_e \cdot 10^4$/ mol g^{-1}	$k_2 \cdot 10^{-3}$/ g mol^{-1} h^{-1}	R^2
T900	120	0.91	13.59	0.968	1.15	0.66	0.960
P900	12	0.08	19.11	0.767	0.19	23.77	0.999
V900	12	0.13	19.81	0.746	0.28	13.63	0.998
TS	168	1.19	16.35	0.854	1.74	0.76	0.976
PS	168	1.25	19.81	0.900	2.00	1.13	0.995
VS	168	1.05	19.58	0.959	1.78	1.14	0.995
M1	168	1.25	12.67	0.938	1.57	0.42	0.943
M2	120	1.18	15.20	0.964	1.81	0.69	0.984
M3	24	0.80	21.88	0.785	1.96	2.69	0.999
M7	168	1.02	17.27	0.923	1.96	1.10	0.991
M8	168	1.09	16.81	0.888	1.87	1.04	0.990
M9	168	1.05	20.04	0.944	1.78	1.17	0.994

630

631

632

633 **Table 6**

Sample	Langmuir			Freundlich		
	$Qo \cdot 10^3$/ mol g^{-1}	$b \cdot 10^{-3}$/ L mol^{-1}	R^2	1/n	$K_F \cdot 10^3$/ / $(mol\ g^{-1})/(mol\ L^{-1})^{1/n}$	R^2
T900	0.22	33.66	0.981	1.11	939.29	0.907
P900	0.00	-0.88	0.897	50.67	∞	0.679
V900	0.02	1.93	0.790	11.44	∞	0.741
TS	-	19.77	0.980	0.25	4.10	0.844
PS	0.72	16.00	0.994	0.35	8.08	0.804
VS	0.52	74.41	0.999	0.10	1.06	0.984
M1	0.80	53.74	0.997	0.26	6.05	0.944
M2	0.41	17.57	0.990	0.26	2.6	0.906
M3	0.85	10.13	0.988	0.34	8.34	0.987
M7	0.61	7.12	0.987	0.26	3.24	0.972
M8	0.92	17.41	0.991	0.29	7.06	0.968
M9	0.50	13.00	0.994	0.27	3.04	0.991

634

635

Fig. 1

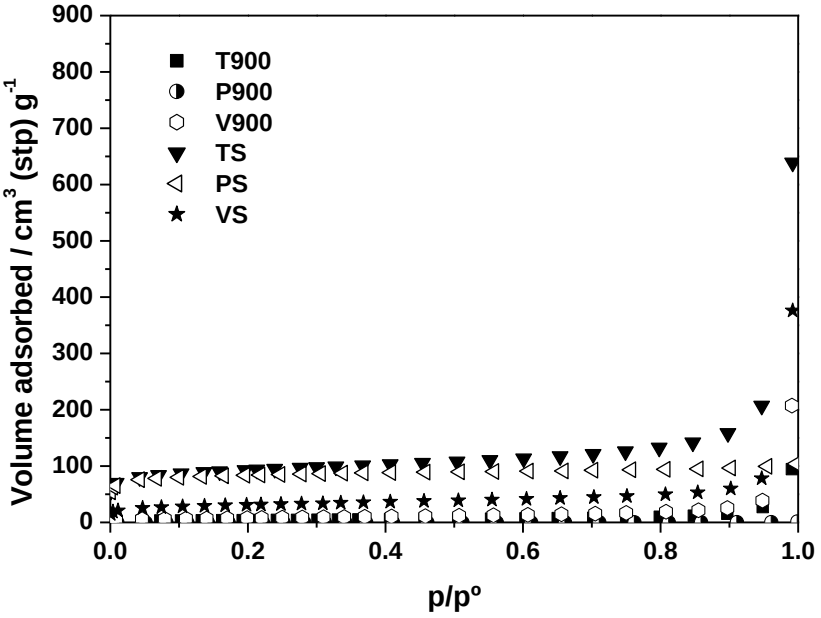
T900
P900
V900
TS
PS
VS
Volume adsorbed / cm3 (stp) g-1
p/p°
0
100
200
300
400
500
600
700
800
900
0.0
0.2
0.4
0.6
0.8
1.0

Fig.2

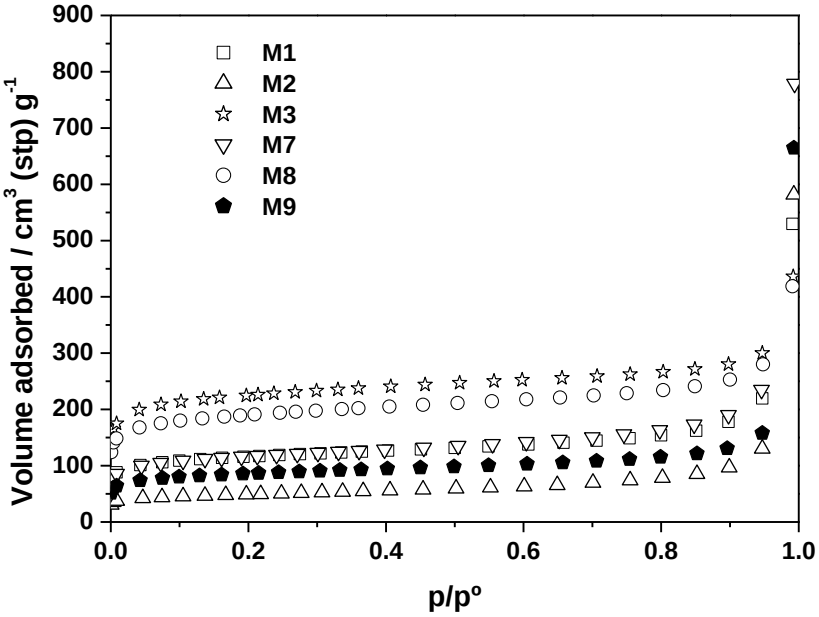

649

650 **Fig. 3**

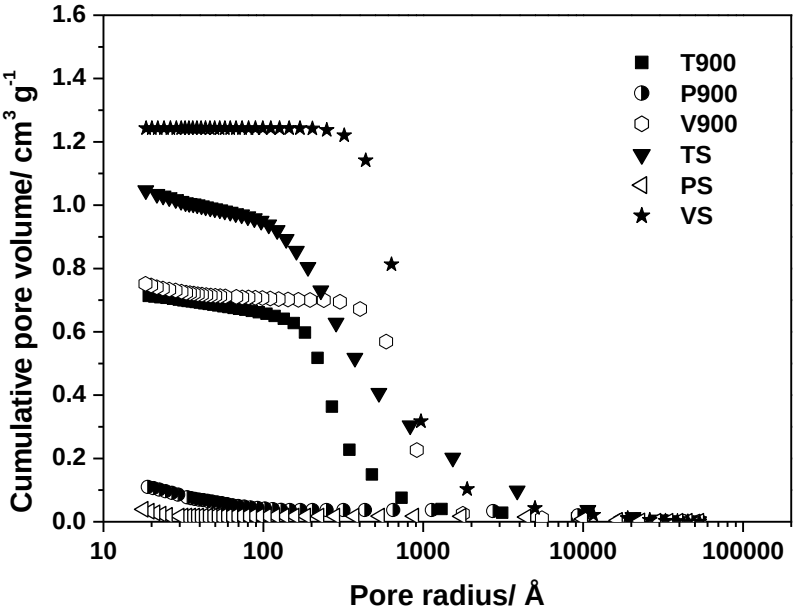

651

652 **Fig. 4**

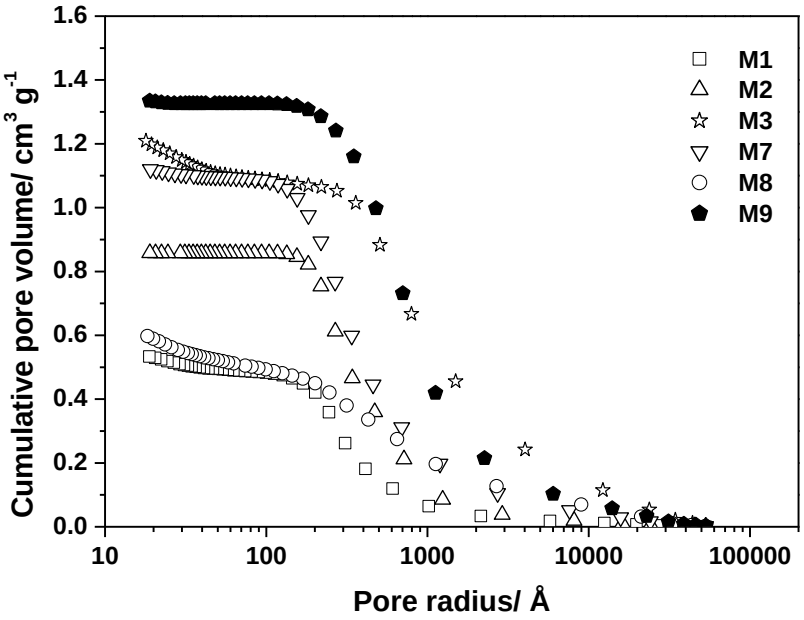
Cumulative pore volume/ cm^3 g^{-1}
Pore radius/ Å
M1
M2
M3
M7
M8
M9
0.0
0.2
0.4
0.6
0.8
1.0
1.2
1.4
1.6
10
100
1000
10000
100000

653

654

655 **Fig. 5**

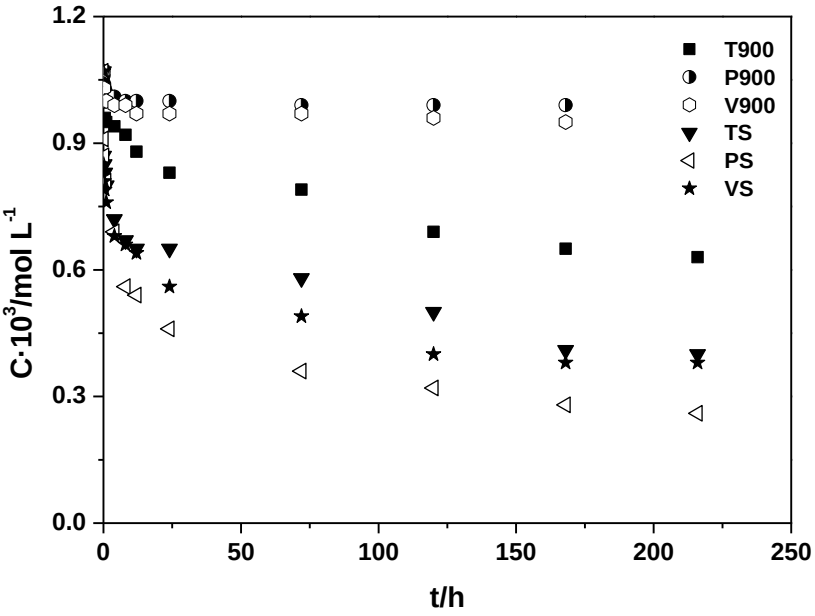

656

657 **Fig. 6**

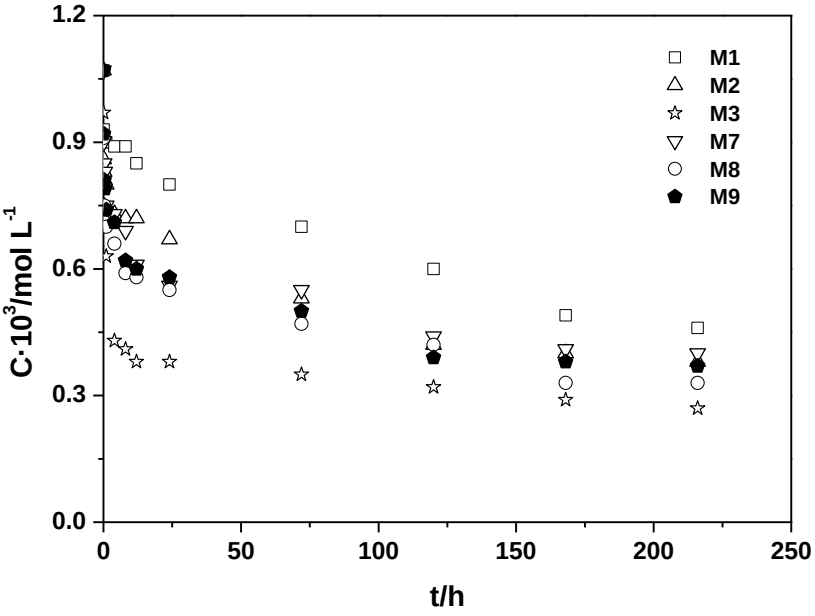

658

659 **Fig. 7**

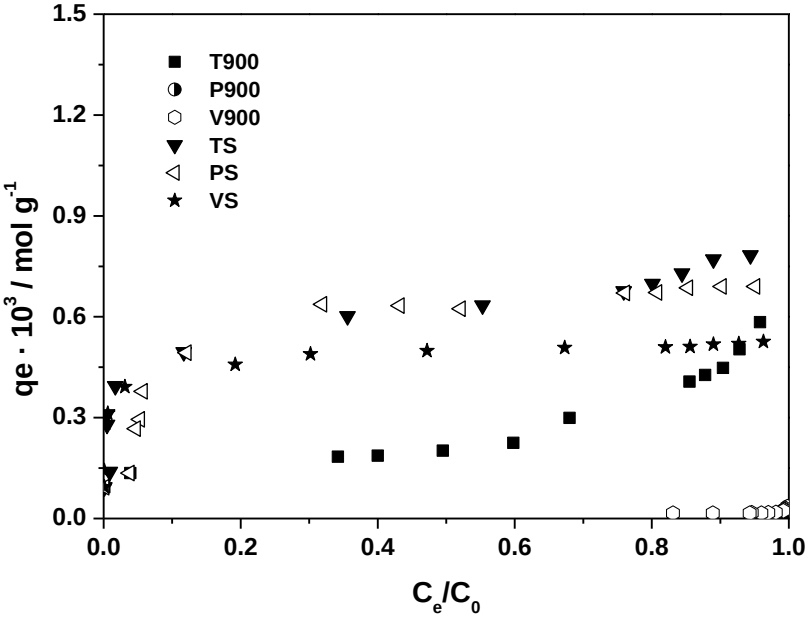

660

661 **Fig. 8**

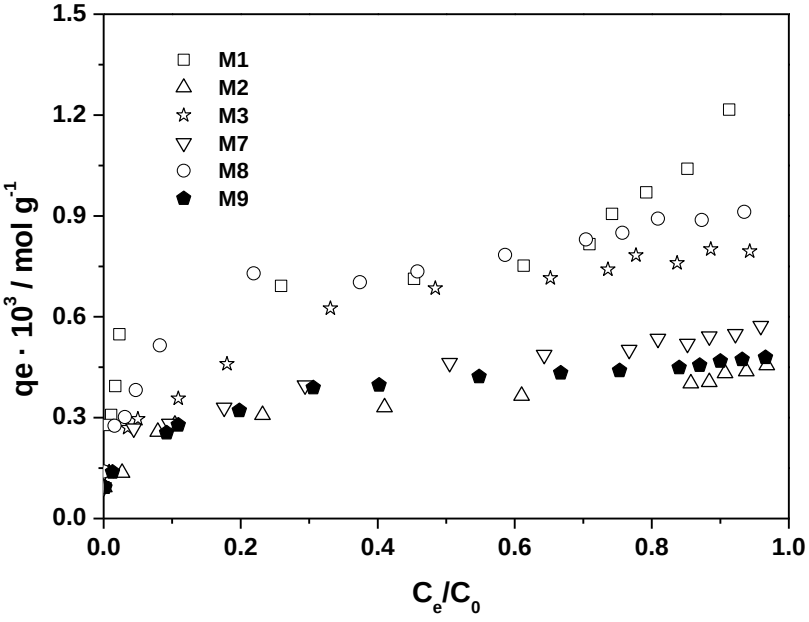

662